The Privileged Status of Peer Faces: Subordinate-level Neural Representations of Faces in Emerging Adults

Junqiang Dai[1] and **K. Suzanne Scherf**[2]

Abstract

■ Faces can be represented at a variety of different subordinate levels (e.g., race) that can become "privileged" for visual recognition in perceivers and is reflected as patterns of biases (e.g., own-race bias). The mechanisms encoding privileged status are likely varied, making it difficult to predict how neural systems represent subordinate-level biases in face processing. Here, we investigate the neural basis of subordinate-level representations of human faces in the ventral visual pathway, by leveraging recent behavioral findings indicating the privileged nature of peer faces in identity recognition for adolescents and emerging adults (i.e., ages 18–25 years). We tested 166 emerging adults in a face recognition paradigm and a subset of 31 of these participants in two fMRI task paradigms. We showed that emerging adults exhibit a peer bias in face recognition behavior, which indicates a privileged status for a subordinate-level category of faces that is not predicted based on experience alone. This privileged status of peer faces is supported by multiple neural mechanisms within the ventral visual pathway, including enhanced neural magnitude and neural size in the neural size in the fusiform area (FFA1), which is a critical part of the face-processing network that fundamentally supports the representations of subordinate-level categories of faces. These findings demonstrate organizational principles that the human ventral visual pathway uses to privilege relevant social information in face representations, which is essential for navigating human social interactions. It will be important to understand whether similar mechanisms support representations of other subordinate-level categories like race and gender. ■

INTRODUCTION

Researchers have proposed that visual object recognition occurs at multiple levels of abstraction that are organized hierarchically (Rosch, 1978). The basic level is "privileged" in recognition for several reasons: The category members share a generalized shape (e.g., all faces have a canonical shape) that is easily identifiable by perceivers; labels for basic-level categories are among the first words learned by infants (e.g., dog, cup); and adults categorize and verify labels for objects fastest at the basic level (Rosch, Mervis, Gray, Johnson, & Boyes-Braem, 1976). Interestingly, most of the work investigating the topographic organization of visual object recognition in the brain also indicates that the basic level is privileged at the neural level. Using a variety of behavioral paradigms during neuroimaging, researchers have consistently observed that faces, common objects, and places elicit different patches of activation throughout the ventral visual cortex, particularly in adult brains (Grill-Spector, Golarai, & Gabrieli, 2008; Grill-Spector, Knouf, & Kanwisher, 2004).

However, visual objects can be recognized at increasingly subordinate-level categories (e.g., adult face, child face), which is especially important for objects of expertise, like faces (Tanaka, 2001; Tanaka & Taylor, 1991). With increasing visuoperceptual expertise, the subordinate-level category can become the most psychologically fundamental or "privileged" level (Tanaka & Taylor, 1991). Behavioral training studies with novel objects reveal that early in the process of learning to individuate novel objects, the basic level is privileged; however, with increased training, expertise in recognizing individual novel objects improves and recognition at the subordinate level becomes as fast and accurate as at the basic level (Gauthier, Williams, Tarr, & Tanaka, 1998). This shift reveals how the visual information that the perceiver attends to for the purpose of recognition changes as a function of experience individuating objects within a category. Despite the wealth of behavioral studies investigating this "subordinate-level shift" in visuoperceputal expertise (Pascalis et al., 2005; Tanaka, Kiefer, & Bukach, 2004; Meissner & Brigham, 2001; Pascalis & Bachevalier, 1998), there is little work assessing how subordinate-level representations are manifested in the brain. The central goal of this study was to evaluate how subordinate-level representations of human faces are organized in the ventral visual pathway.

Psychological Relevance of Subordinate-level Categories of Human Faces

In adults, the psychological relevance of subordinate-level categories of human faces, including race and gender, is reflected in patterns of bias in recognition abilities. For

[1]University of North Carolina at Chapel Hill, [2]The Pennsylvania State University, University Park

Journal of Cognitive Neuroscience 35:4, pp. 715–735
https://doi.org/10.1162/jocn_a_01966

example, adults often exhibit superior abilities to recognize faces of individuals from within their own compared with within another race (i.e., the "own race effect"; Hugenberg, Young, Bernstein, & Sacco, 2010; Tanaka et al., 2004; Meissner & Brigham, 2001; Levin, 1996), and to a lesser extent, within their own compared with another gender (i.e., "own-gender bias"; Wright, Boyd, & Tredoux, 2003; Lewin & Herlitz, 2002). There is also evidence that the general age of a face may organize subordinate-level representations of faces, although the patterns of bias in recognition abilities are quite complex. There are examples of an "own-age bias" in recognition abilities of adults (e.g., Wright & Stroud, 2002), but also superior processing of faces from other age groups, including maternity-ward nurses recognizing newborn faces (e.g., Cassia, Picozzi, Kuefner, & Casati, 2008) and young children recognizing adult faces (i.e., "caregiver bias"; Picci & Scherf, 2016). These biases reflect that faces can be represented at a variety of different subordinate levels, which can become "privileged" for visual recognition in perceivers.

The mechanisms influencing the privileged status of subordinate-level representations of faces are likely varied, reflecting visuoperceptual experience (Tanaka, 2001; Diamond & Carey, 1986; Brigham & Malpass, 1985), social motivation (Hugenberg et al., 2010), and/or the primacy of social developmental tasks (Picci & Scherf, 2016; Scherf & Scott, 2012), and may change as a function of development (Scherf & Scott, 2012). As a result, it has been difficult to make strong predictions about how neural systems represent these subordinate-level biases in face processing.

Neural Representation of Subordinate-level Categories of Human Faces

There is a large literature investigating the neural representation of faces at both the basic (face vs. object) and even individual (Marilyn vs. Maggie) levels. When defined at the basic level (e.g., faces vs. common objects), faces activate a broad network of regions that extend throughout the ventral temporal pathway including the occipital face area (OFA), posterior fusiform gyrus, the fusiform face area (FFA), and the anterior temporal pole, but also include the amygdala, ventromedial prefrontal cortex, posterior parietal cortex, and posterior superior temporal cortex in both hemispheres (Haxby, Hoffman, & Gobbini, 2002; Haxby et al., 2000). At the exemplar, or individual, level, the topography of activation does not vary as much as the patterns of activation within specific regions of the face-processing network. For example, using a multivariate analytic approach, researchers determined that regions in the bilateral fusiform gyri and anterior middle temporal gyri represent face identity (Nestor, Plaut, & Behrmann, 2011). Critically, the regions in the fusiform gyrus that were identified in this multivariate approach were not face-selective regions, meaning that they were not identified in a basic-level contrast (i.e., faces vs. objects). This finding may indicate that representations for faces at the basic and exemplar levels are differentiated, in part, by the locus of activation within the fusiform gyrus.

Compared with these basic- and individual-level studies of neural representation, there is a relative dearth of studies evaluating how the brain represents subordinate-level categories of faces. Most studies investigating the neural basis of subordinate-level face representations have focused on understanding how the brain represents own- versus other-race faces or the gender of faces. Many of these studies have reported differences in the magnitude and/or pattern of activation between the different subcategories of faces within regions of the face network (for a review, see Kubota, Banaji, & Phelps, 2012). One study reported that the right and left FFAs encode difference race faces as a function of differential patterns of activation (Contreras, Banaji, & Mitchell, 2013). The same authors reported that the bilateral FFA also encodes gender via differential patterns of activation (Contreras et al., 2013). Other studies of face gender have reported a similar finding of differential patterns of activation throughout multiple regions in the face-processing network (e.g., Kaul, Rees, & Ishai, 2011).

There are far fewer studies investigating age as a subordinate level for organizing face representations in the brain. In one study, young adults (~23 years old) categorized unfamiliar peer-aged (~22 years old) and older-aged (~75 years old) faces by age and gender while being scanned (Wiese, Kloth, Güllmar, Reichenbach, & Schweinberger, 2012). Although participants were faster to categorize older faces than peer faces, there were no differences in the magnitude of activation (i.e., percentage signal change) related to the age of the face stimuli in any of the regions within the face-processing network that they investigated (bilateral FFA and OFA). In another study, children (ages 7–10 years) and adults (ages 18–40 years) performed a simple recognition memory task separately for adult and child faces (Golarai, Liberman, & Grill-Spector, 2017). There were no differences in the recognition accuracy for either face age or as a function of either age group. However, the adults exhibited reliably different patterns of activation throughout the ventrotemporal cortex during recognition of the adult and child faces, whereas the children did not. Altogether, the work investigating the neural basis of race, gender, and age as relevant dimensions of subordinate-level representations of faces provides inconsistent information regarding the mechanism for encoding faces at this level.

Current Study

To investigate the neural basis of subordinate-level representations of human faces in the ventral visual pathway, we leveraged recent behavioral findings indicating the privileged nature of peer faces in identity recognition for adolescents and emerging adults (EAs; Picci & Scherf, 2016). In this work, peer faces are defined not just by age, but also by social developmental tasks (e.g., finding a mate, creating a family, raising a family) that are related to, but not yoked to, age. Adolescence, roughly the second decade of life, and emerging adulthood (~18–25 years; Arnett, 2000) represent developmental periods of increasing autonomy from the familial unit and in which affiliative relationships become reorganized to focus on peers (Havighurst, 1972). Previously, we proposed that these social developmental tasks (e.g., autonomy from familial unit, developing peer relationships) fundamentally shape the computational goals of the perceptual system, which are ultimately reflected in face-processing biases (Scherf & Scott, 2012; Scherf, Behrmann, & Dahl, 2012). We reported that a *peer bias* (i.e., superior recognition for peer compared with other faces) emerges in adolescence and becomes prominent in the face recognition behavior of EAs (Picci & Scherf, 2016). Specifically, EAs exhibit superior recognition of EA faces compared with the other kinds of faces, whereas adolescents exhibit superior recognition of adolescent faces compared with the other groups of faces. Given the strength of these behavioral findings, we used a similar paradigm to investigate the neural basis of the peer bias in the face recognition behavior of EAs (age 18–22 years) who are expected to exhibit a prominent behavioral peer bias in their face recognition abilities.[1]

Specifically, we evaluated the presence of a potential peer bias in face identity recognition behavior among 166 EAs in the context of recognizing child, early puberty adolescent, late puberty adolescent, EA (i.e., peer), and faces of individuals that would be approximately the age of the parents of the EA participants (i.e., parent-aged [PA] faces). To assess the neural basis of subordinate-level representations of all these face categories and determine whether any of them is privileged in the brains of EAs, we scanned a subset of these participants using fMRI in two paradigms. In the first paradigm, we employed a visual stimulation task to map the topography of neural responses to each of these subordinate-level faces in the ventral visual pathway (i.e., child, early adolescent, late adolescent, EA, and PA faces). We hypothesized that the locus, size of regions activated, and/or magnitude of activation within the regions may differentiate the subcategories of faces, and particularly peer faces. In a second task, participants engaged in a 1-back recognition memory task for faces from each subordinate-level category. This task was used to specifically measure BOLD activation during the process of face identity recognition. Given the previously observed peer bias in face recognition behavior, we predicted that the magnitude of responses would differentiate the peer compared with the other aged faces among regions in the face-processing network.

METHODS

Participants

Typically developing EAs (n = 166, M_{age} = 19.7 years, SD = 1.9 years; 57% female; see Table 1) were tested in the behavioral portion of the experiment. Participants were healthy with no history of neurological or psychiatric disorders in themselves or their first-degree relatives. They were screened for behavioral symptoms indicative of undiagnosed psychopathology. A total of 35 participants were excluded because of experimenter error or because their average total performance was below chance (i.e., accuracy is below 50%; n = 12). As a result, the final sample included 131 participants (M_{age} = 19.5, SD = 1.7 years; 60% female; see Table 1). A subset of 31 EAs (M_{age} = 19.3 years, SD = 1.3 years; 52% female; see Table 1) was scanned in the fMRI study. These individuals were selected into the fMRI study because of their interest in participating and their ability to pass the MRI safety screening procedures, without regard for their behavioral performance. This included no history of head injuries or concussions, normal or corrected vision, and they were all right-handed. The sample size for the behavioral study was based on our recent behavioral study that at least 28 individuals were required to give us 80% power to detect a moderate sized effect (i.e., 0.5) at a significance level of 0.05 (Picci & Scherf, 2016). The sample size for the neuroimaging studies was based on previous studies in which experimental effects were observed in face-processing network using a similar blocked design (Scherf, Elbich, & Motta-Mena, 2017; Scherf, Elbich, Minshew, & Behrmann, 2015).

Written informed consent was obtained using procedures approved by the institutional review board of The Pennsylvania State University. Participants were recruited through the Psychology Department undergraduate subject pool and via fliers on campus.

Measures

Peer Bias Behavioral Task

To investigate the peer bias in face recognition memory in EAs, we adapted the old/new face-memory task that we developed previously (Picci & Scherf, 2016). We included all four of the original face category stimuli (i.e., 6- to 8-year-old children, 11- to 14-year-old early-puberty (EP) adolescents, 11- to 14-year-old late-puberty (LP) adolescents, and sexually mature 18- to 20-year-old EAs) from our previous paradigm (Picci & Scherf, 2016). In addition, we added a fifth block of faces that represented the current age of parent faces to the EA participants, that is, individuals who are between the ages of 40–50 years of age. We call this developmental group "PA" faces because of their relative developmental relation to the EA participants, not because we confirmed that the individuals did indeed have children of their own.

Table 1. Participant Demographics

Sample	*n*	*Age, years (SD)*	*% Female*
Behavioral testing	166	19.7 (1.9)	57
fMRI testing	31	19.3 (1.3)	52

The stimuli consisted of 150 grayscale photographs of faces with neutral and happy expressions (see Figure 1A). There were 30 images from each of five face subcategories that corresponded to each developmental group: (6- to 8-year-old children, 11- to 14-year-old EP adolescents, 11- to 14-year-old LP adolescents, sexually mature 18- to 20-year-old EAs, and sexually mature 40- to 50-year-olds). We collected perceived pubertal status of the adolescent faces from an independent group of EA participants and verified that the status ratings were significantly different across all categories (e.g., child < all others; early puberty adolescent < late puberty adolescent < EA). The racial/ethnic composition of the faces in the stimuli reflected the racial/ethnic distribution of the town where we recruited participants. For each face category, there were an even number of male and female target and distractor identities. There were two separate images of each target identity, one presented at encoding and the other at test (see Figure 1A).

Photographs were obtained from multiple face databases: NimStim (Tottenham et al., 2009), Karolinska (Lundqvist, Flykt, & Öhman, 1998), National Institute of Mental Health (NIMH) Child Emotional Faces Picture Set (Egger et al., 2011), JimStim (Tanaka & Pierce, 2009), and the Radboud Face Database (Langner, Dotsch, Bijlstra, Wigboldus, Hawk, & van Knippenberg, 2010). In addition, approximately 50% of the images of LP adolescents and 50% of images of parents were taken in the Laboratory of Developmental Neuroscience at The Pennsylvania State University. Extreme blemishes or scars were masked to eliminate artificial cues to recognition. Hair and clothing were not cropped out of the images. All images were presented on a black background and were standardized for luminance and image size.

Face-recognition abilities were measured using a computerized game. After studying 10 target faces, participants identified whether each face in a set of 20 faces (10 targets, 10 distractors) was in the study group ("old") or not ("new"). The task was presented in blocked design with each block containing face stimuli for one of the five face categories. The order of the blocks was counterbalanced across participants. Participants first completed a practice session, which consisted of an abbreviated version of each phase of the task. At the end of the practice, participants were instructed to remember the person and not the picture to encourage them to create an invariant representation of the face identity. This task has good external validity with other tests of unfamiliar face identity recognition, including both the Male and Female Cambridge Face Memory Long Form Tests (see Arrington, Elbich, Dai, Duchaine, & Scherf, 2022).

Each task block was divided into three sections, encoding, delay, and recognition. During the encoding phase, participants were presented with the target faces and told that these were the faces of people who were going into a movie; each face had a neutral expression. Participants had 2000 msec to encode each face. In the delay period, all participants watched a movie trailer (~90 sec). During the test phase, participants were presented with the 10 target faces, except now each target face exhibited a smiling expression. These target faces were shown together with 10 distractor faces, which were also smiling. By presenting perceptually transformed images of the target faces during the test phase, we were able to assess participants' invariant representation of face identity rather than image-specific memory. Each face was presented for 3000 msec. Participants responded "yes" ("I recognize this face") or "no" ("I do not recognize this face") by pressing a key. Participants were instructed to perform as quickly and accurately as possible.

MRI Acquisition

Before scanning, all participants were placed in a mock MRI scanner for approximately 20 min and practiced lying still. This procedure is highly effective at acclimating participants to the scanner environment and minimizing motion artifact and anxiety (Scherf, Thomas, Doyle, & Behrmann, 2014). Participants were scanned using a Siemens 3 T Trio MRI scanner with a 12-channel phase array head coil at the Social, Life, and Engineering Imaging Center at The Pennsylvania State University. During the scanning section, the stimuli were displayed on a rear-projection screen located inside the MR scanner.

Functional EPI images were acquired in 34, 3-mm-thick slices that were aligned approximately 30° perpendicular to the hippocampus, which is effective for maximizing signal in the medial temporal lobes (Whalen et al., 2008). This scanning protocol allowed for complete coverage of the medial and lateral temporal lobes, frontal, and occipital lobes. For individuals with larger head size, some of the superior parietal lobe was not scanned. The scan parameters were as follows: 3-mm isotropic voxels; repetition time = 2000; echo time = 25 msec; field of view = 210 × 210; matrix 70 × 70; flip angle = 80°. High-resolution anatomical images were also collected using a 3-D magnetization prepared rapid gradient echo with 176 $1 mm^3$, T1-weighted, straight sagittal slices (repetition time = 1700; echo time = 1.78; flip angle = 9°; field of view = 256).

Visual stimulation task. A visual stimulation task was created to activate face-selective regions in individual participants. Tasks with dynamic stimulation are better at eliciting face-related activation throughout multiple nodes of the distributed face-processing network (Pitcher, Walsh, & Duchaine, 2011; Fox, Iaria, & Barton, 2009). Given that our goal was to investigate the possibility that subordinate-level category information is represented in multiple nodes of the face-processing network, we employed a dynamic task that would provide a better chance of identifying activation throughout this distributed network.

This task contained two runs and included blocks of silent, fluid concatenations of short movie clips downloaded from the Internet. The short (3–5 sec) video clips in the stimulus blocks were taken from YouTube and

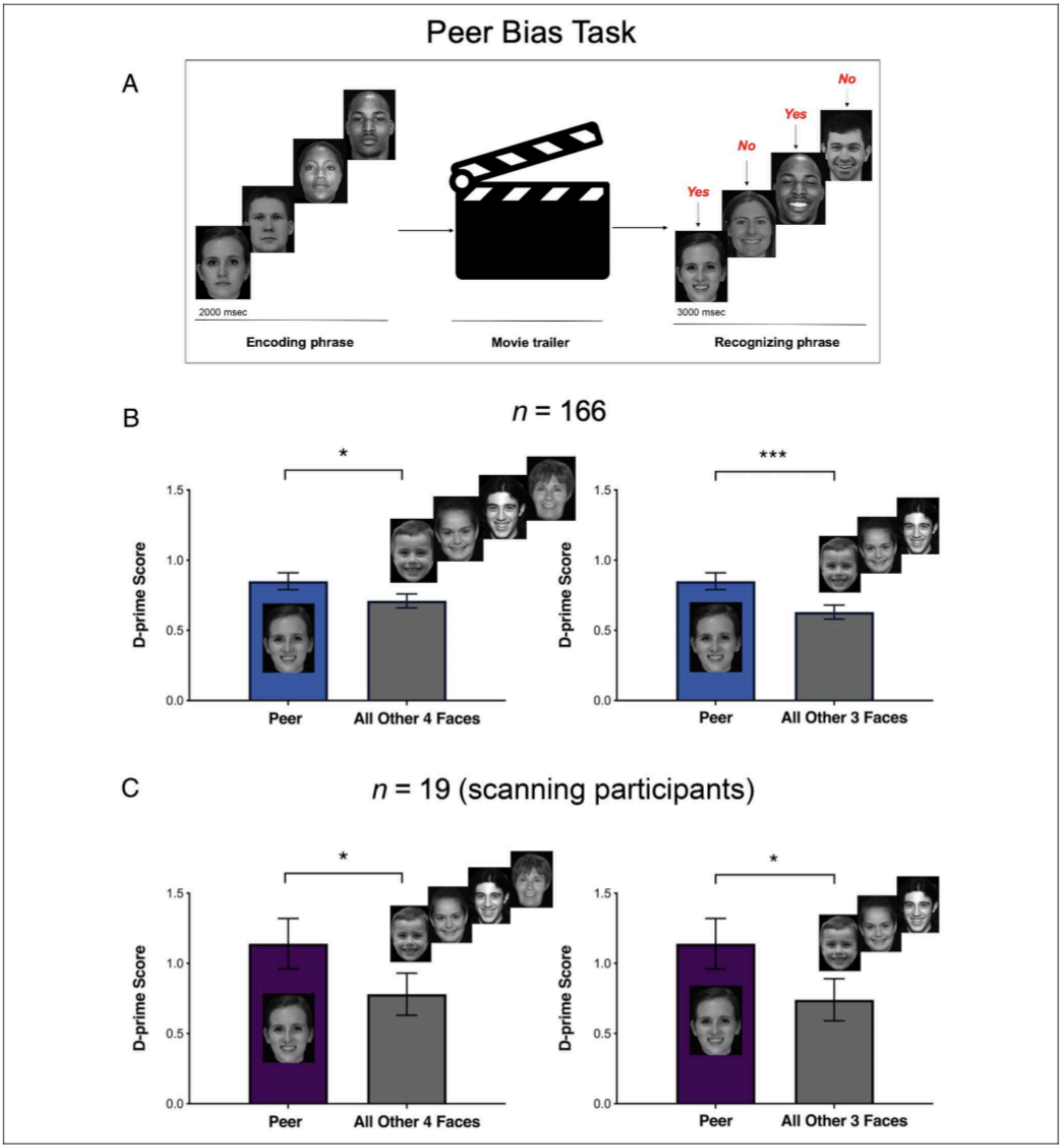

Figure 1. Face recognition behavioral task and performance. (A). Example of face identity recognition behavioral task from the emerging adult faces block. Each task block was divided into three sections, encoding, delay, and recognition. During the encoding phase, participants were presented with 10 target faces for 2000 msec each and asked to remember them. In the delay period, all participants watched a trailer for a movie (~90 sec). During the recognize phrase, participants were presented with 10 target and 10 distractor faces, all of whom exhibited a smiling expression, and were asked to determine whether the face was "old" or "new." Behavioral performance as a function of face subcategory for (B) all participants (n = 166). (C) Individuals who also participated in the scanning experiment (n = 31). The data figures represent the distribution of d' scores for each face condition across participants. The plot shows the means (bars) ± 1 standard error (*SE*). Peer = emerging adult faces condition. "All Other 4 Faces" represents the average performance across the child, early pubertal adolescent, late pubertal adolescent, and parent-aged face conditions. "All Other 3 Faces" represents the average performance across the child, early pubertal adolescent, and late pubertal adolescent face conditions; we include these results to replicate our previous behavioral findings (Picci & Scherf, 2016).

edited together using iMovie. Movies of objects included moving mechanical toys and devices (e.g., dominos falling) and were used in our previous work (Elbich, Molenaar, & Scherf, 2019; Elbich & Scherf, 2017). The movie clips of faces were intensely affective (e.g., a person laughing or crying) to elicit activation throughout the network of core and extended face processing regions (Gobbini & Haxby, 2007). Videos from all five face categories were represented in this task, including children, EP adolescents, LP adolescents, EAs, and PA individuals. The face movies included an even number of unfamiliar male and female actors expressing positive (e.g., happy, joyful, or enthusiastic) or negative (e.g., angry, scared, or crying) emotion (see Figure 2A). The movie clips were rated for emotional intensity in a separate group of EA participants. The movie clips were balanced across subcategory for emotional intensity.

In total, there were eighteen 16-sec stimulus blocks. In each run, there were three 16-sec blocks for each condition. (i.e., 6/conditions). Each run lasted 7 min 12 sec, which began and ended with 12-sec fixation blocks. The order of the stimulus blocks was randomized for each participant. Fixation blocks (6 sec) were interleaved between task blocks. After the first fixation block in each run, there was a 12-sec block of patterns. The order of the two runs was counterbalanced across participants.

Participants were instructed to watch the movies and be still. Therefore, there were no constraints on the kind of processing that was engaged by participants in response to the stimuli; it was not focused on identity recognition or any other process (e.g., emotion categorization, gender or age evaluation). The task was designed so that large ROIs could be identified and characterized within individual participants.

fMRI face recognition task. This task was specifically designed to engage face identity recognition processes because the peer bias is manifested in recognition behavior. When creating this task, we balanced the needs to evince a peer bias in activation and maximize the signal-to-noise ratio in a novel paradigm in regions that are susceptible to sinus artifact (e.g., amygdala, anterior temporal lobe [ATL]). As a result, we settled on a 1-back memory task for face identity in a blocked fMRI design using static images. Although the *n*-back was originally designed to engage working memory processes, the 1-back version has been used successfully to engage face identity recognition processes in which participants must invoke a mental representation of face

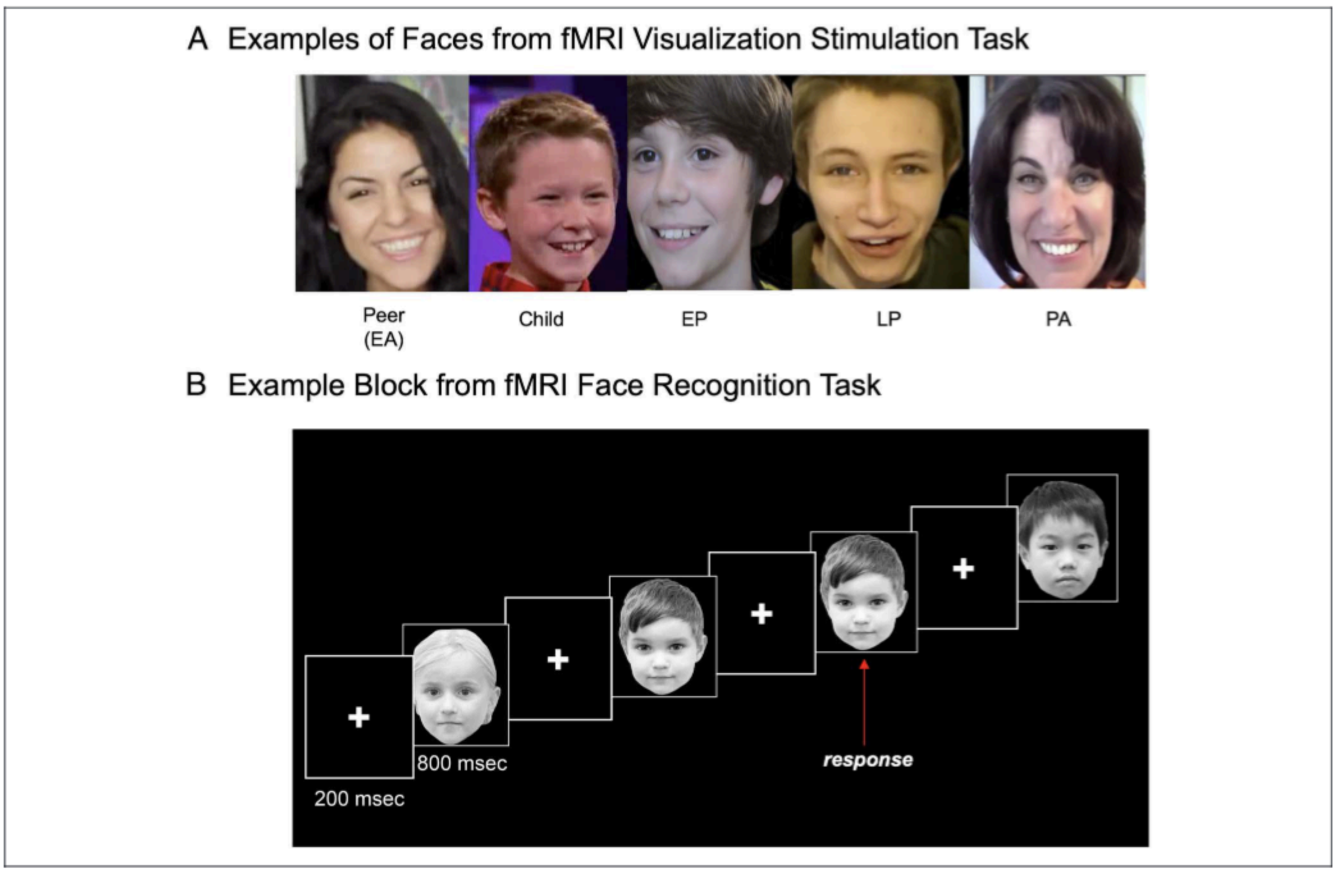

Figure 2. Neuroimaging tasks. (A). Examples of face categories in the visual stimulation task. Movie clips for each of five face conditions were included in the task including peer (i.e., emerging adult), child, early pubertal (EP) adolescent, late pubertal (LP) adolescent, and parent-aged (PA) adult. The emotional intensity of the movie clips was matched across conditions. (B). Example block of fMRI face recognition task. The 1-back recognition task was executed in separate blocks for each of the five face subcategories as defined in the visual stimulation task (block orders were randomized). This is an example of the stimuli from the child face 1-back block.

identity in the absence of a percept (e.g., Herrington, Riley, Grupe, & Schultz, 2015; Gauthier et al., 2000; Kanwisher, Tong, & Nakayama, 1998).

Participants saw images of common objects and faces from each of the five developmental categories (i.e., child, EP adolescent, LP adolescent, peer–EA, PA faces). The face images used in this experiment were selected from several databases including Child Affective Facial Expression (LoBue & Thrasher, 2015), JimStim (Tanaka & Pierce, 2009), NIMH Child Emotional Faces Picture Set (Egger et al., 2011), Center for Vital Longevity Face (Minear & Park, 2004), NimStim (Tottenham et al., 2009), and Karolinska (Lundqvist et al., 1998). Common objects (inanimate objects) were downloaded from the Internet. The size (300 pixels/in.), color (gray scale), and luminance of the images were controlled using Photoshop.

The task was a single run block design with six 12-sec blocks of each visual category, the order of which was randomized for each participant, interleaved with 6-sec fixation blocks. Within each task block, 12 images were each presented for 800 msec followed by a 200-msec fixation. Participants completed a 1-back task while viewing the pictures and responded by button press when they saw a picture repeat (see Figure 2B). Two images repeated in each stimulus block, the order of which was counterbalanced across blocks. Accuracy was collected as a measure of task performance. The duration of the task was 9 min 36 sec.

Data Analyses

Peer Bias Behavioral Data

We converted the accuracy data to d' scores. We used the loglinear approach to compute the hit and false alarm rates as follows (Stanislaw & Todorov, 1999).

$$\begin{cases} \text{①}\ \text{Hit Rate } (H) = \dfrac{Hits + .5}{Total\ Hits + 1} \\ \text{②}\ \text{False Alarm}(FA) = \dfrac{(FA + .5)}{Total\ FA + 1} \\ \text{③}\ d' = z(H) - z(FA) \end{cases}$$

Before analyses, a process template was designed and coded for data cleaning and processing at the individual participant level. The raw data from each participant were downloaded onto this process template to identify trials with outlier RTs. We determined the minimum RT threshold by averaging RT on the fastest five accurate trials across all participants (50 msec). The maximum RT threshold was 2950 msec (i.e., 50 msec under the max trial time). Therefore, any trials with RT less than 50 msec or greater than 2950 msec were removed from the analysis for each participant. The corresponding hit or false alarm rates were adjusted to accommodate the removal of each trial. Data from the entire task were removed from the analysis if the average total accuracy across all conditions was below chance (i.e., $< 50\%$; $n = 12$) or whose average d' score across conditions indicated confusion executing the task (i.e., $d' < -1$; $n = 19$). Finally, to address outlier data points, we Winsorized the d' values separately for each face condition (e.g., Picci & Scherf, 2016).

Planned comparisons were evaluated using paired-samples t tests. Specifically, we predicted that recognition performance for peer faces (i.e., EA faces) would exceed performance for all other faces (average of other face categories—see Picci & Scherf, 2016). However, because we added the PA faces in the paradigm, we computed two estimates of "other faces" for each participant. First, we computed the average performance in response to the child, and both groups of adolescent faces to directly compare these findings with our prior results (Picci & Scherf, 2016). Second, we computed the average performance in response to all other face categories, including PA faces.

fMRI face recognition task behavioral data. Because of the relatively limited number of potential hits (i.e., 2) compared with false alarms (i.e., 8) in each block, we did not convert the accuracy data from the scanner face recognition task into d' scores. To compute accuracy for each face subcategories, we adopted a strategy like signal detection theory. Specifically, in addition to assessing accuracy on the target present trials, we also assessed accuracy on the target absent trails. So, if a participant pressed the response button for a nontarget trial, it counted as a false alarm and, thus, an incorrect trial for the analysis.

Neuroimaging Data

Defining individual face-related ROIs. Imaging data were analyzed using Brain Voyager QX version 2.3 (Brain Innovation). Preprocessing of functional data included 3-D motion correction and filtering out low frequencies (three cycles). Only those participants who exhibited maximum motion of less than 2/3 of a voxel in all six directions (i.e., no motion greater than 2.0 mm in any of six motion vectors on any image in all runs of both tasks) were included in the fMRI analyses. No participant was excluded because of excessive motion.

For each participant and each task, the time-series images for each brain volume were analyzed separately for basic and subordinate-level category differences (e.g., objects, child faces, EP adolescent faces, LP adolescent faces, peer faces, and PA faces) in a fixed-factor general linear model (GLM). The GLM was computed on the z-normalized raw signal in each voxel. Each stimulus category was defined as a separate predictor and modeled with a box-car function, which was convolved with a canonical hemodynamic response to accommodate the delay in BOLD response. The time-series images were then spatially normalized into Talairach space. The functional images were not spatially smoothed (Grill-Spector & Weiner, 2014).

Face-related activation was defined separately for each participant for each subordinate-level face category using a whole-brain contrast (e.g., child faces – objects; peer faces – objects) that was corrected for false positive activation at the whole-brain level using the false discovery rate with $q < 0.10$ (Genovese, Lazar, & Nichols, 2002). This generated activation maps for each participant including a child face map, an EP adolescent face map, an LP adolescent face map, a peer face map, and a PA face map. From *each* activation map, we defined face-related functional ROIs in each individual participant that were inspired by the Gobbini and Haxby (2007) model of face processing. These ROIs included core (e.g., OFA, FFA1, posterior superior temporal sulcus [pSTS]) and extended (e.g., amygdala, ATL) regions in each hemisphere. The cluster of contiguous voxels nearest the classically defined fusiform area (FFA) in the middle portion of the gyrus was identified as the pFus-faces/FFA1 (Weiner & Grill-Spector, 2010). We defined the OFA as the set of contiguous voxels on the lateral surface of the occipital lobe closest to our previously defined adult group level coordinates (x, y, z coordinates: 50, −66, −4; Scherf, Behrmann, Humphreys, & Luna, 2007). The pSTS was defined as the set of contiguous voxels within the horizontal posterior segment of the superior temporal sulcus that did not ascent into the posterior segment of the STS. The most anterior boundary of the pSTS was where the ascending segment of the intraparietal sulcus (IPS) intersected the lateral fissure. The ATL ROI was defined as the cluster of voxels nearest the coordinates reported previously in studies of individual face recognition (Mur, Ruff, Bodurka, Bandettini, & Kriegeskorte, 2010), which is at the most anterior tip of the collateral sulcus and fusiform gyrus, between the occipitotemporal sulcus and the parahippocampal gyrus. The amygdala was defined as the entire cluster of face-selective voxels within the gray matter structure. Any active voxels that extended beyond the structure out to the surrounding white matter, horn of the lateral ventricle, or hippocampus were excluded.

Defining individual early visual cortex ROIs. We defined early visual cortex (EVC) in each individual in each hemisphere separately to evaluate as control regions. Functional activation in EVC was defined using a whole-brain contrast (objects–fixation) that was corrected for false positive activation at the whole-brain level using the false discovery rate with $q < 0.05$ (Genovese et al., 2002). Following Nishimura and colleagues (Nishimura, Scherf, Zachariou, Tarr, & Behrmann, 2015), EVC was identified in each hemisphere separately in the most ventral axial slice of the occipital pole in which the calcarine sulcus could be visualized. We selected activation posterior to the calcarine sulcus on the axial slice and included contiguous voxels of activation that extended a maximum of 10 mm above or below the axial slice in which the calcarine sulcus was identified. We used the transverse occipital sulcus as the lateral boundary for activation.

ROI-based Analyses

Visual stimulation task. Table 2 illustrates the total number of participants for whom each ROI was definable together with the average coordinates of the centroid of each region. The ROIs were quantified in terms of the total number of significantly active voxels. A score of 0 was entered if a participant did not exhibit any significantly active voxels for a given ROI. Only ROIs in which a minimum of 50% of the participants had definable functional ROIs for all five categories were selected for additional analyses. This included bilateral FFA1, right OFA, and right pSTS. There was not enough data to include the bilateral amygdala, anterior temporal poles, left OFA, or left pSTS in additional analyses.

The data that were analyzed for the effects of subordinate-level representation are shown in Table 3. These data were not normally distributed; therefore, we used a square root transformation before analyses (Elbich & Scherf, 2017). Planned contrasts were conducted to compare the size of ROIs activated by peer faces versus those from the other face subcategories (i.e., average of child, EP, LP, and PA face ROIs). We also report the 95% confidence intervals of the difference scores.

To compute the magnitude of subcategory selectivity within each region, separate ROI-based GLMs were conducted for each participant in each ROI. This generated beta weights for each subcategory for each participant from each map. Participants with no definable voxels in an ROI were excluded from the statistical analyses for neural magnitude, given that no beta weights could be extracted from ROI-based GLM. The goal was to evaluate whether a functionally defined ROI that was selective for

Table 2. Number of Definable Face-selective ROIs for Each Subordinate-level Face Category from Visual Stimulation Task

	Child	*EP*	*LP*	*EA*	*PA*
rFFA1	27	26	28	27	26
lFFA1	27	26	26	25	23
rOFA	16	17	18	22	16
rpSTS	21	24	20	23	22
rAmygdala	5	12	10	7	8
lAmygdala	7	8	11	8	10
rATL	12	18	13	12	10
lATL	13	14	12	12	10
lOFA	12	17	16	21	16
lpSTS	12	21	19	19	22

Each functional ROI in this table was defined as relevant face category versus object (e.g., child vs. object). EP represents early pubertal adolescent face, LP represents late pubertal adolescent face, EA represents emerging adult face, and PA means parent-aged face condition. There are 31 participants in this study. We focused on the core and extended face neural network and defined these bilateral ROIs. To ensure the power of analysis, only those ROIs in which more than half of participants (i.e., > 16) had significant activation were included in final statistical analyses (i.e., rFFA1, lFFA1, rOFA, and rpSTS). r = right; l = left; FFA = fusiform area; OFA = occipital face area; pSTS = posterior superior temporal sulcus; ATL = anterior temporal lobe.

Table 3. Functional ROIs for Each Face Category from Visualization Stimulation Task

			x	*y*	*z*
ROIs (Defined Maps)	*Size of ROI (SE)*	*n*	*Mean (SE)*	*Mean (SE)*	*Mean (SE)*
rFFA1					
Child	597.42 (211.54)	27	39 (0.58)	−51 (1.35)	−17 (0.77)
EP	516.19 (207.67)	26	39 (0.77)	−50 (1.35)	−18 (0.77)
LP	716.82 (227.38)	28	38 (0.58)	−50 (1.54)	−17 (0.77)
EA	828.35 (148.31)	27	39 (0.77)	−51 (1.54)	−17 (0.77)
PA	488.74 (153.94)	26	38 (0.77)	−52 (1.35)	−18 (0.77)
lFFA1					
Child	519.42 (191.85)	27	−37 (0.60)	−50 (1.60)	−18 (0.80)
EP	557.44 (221.41)	26	−39 (0.80)	−51 (1.80)	−18 (0.60)
LP	600.32 (226.02)	26	−40 (0.60)	−48 (1.60)	−19 (0.60)
EA	655.16 (163.07)	25	−39 (0.60)	−51 (1.80)	−18 (0.60)
PA	409.75 (154.33)	23	−40 (0.60)	−50 (1.60)	−17 (0.60)
rOFA					
Child	109.35 (63.39)	16	29 (2.62)	−86 (2.14)	−4 (2.38)
EP	368.90 (210.92)	17	25 (2.86)	−83 (2.38)	−4 (2.86)
LP	600.76 (278.59)	18	27 (3.33)	−84 (2.38)	−7 (1.90)
EA	597.87 (175.51)	22	27 (2.62)	−87 (1.67)	−10 (1.67)
PA	322.23 (159.74)	16	24 (2.62)	−87 (1.67)	−9 (2.14)
rpSTS					
Child	282.35 (93.25)	21	50 (1.28)	−50 (1.92)	8 (1.28)
EP	583.48 (177.06)	24	51 (1.07)	−48 (1.92)	9 (1.28)
LP	803.29 (211.04)	20	53 (0.64)	−48 (1.71)	8 (0.85)
EA	739.77 (208.94)	23	52 (1.28)	−49 (2.13)	7 (1.07)
PA	449.36 (158.22)	22	51 (1.07)	−49 (1.92)	8 (1.28)

Each face-selective ROI was defined using the contrast (face subcategory vs. objects) during the visual stimulation task and was corrected for FWE using the false discovery rate procedure. The average size and coordinates of the individually defined functional ROIs for each face subcategory. The size of the average ROIs is reported in number of contiguously active voxels. The average coordinates were based on the centroid of the individually defined functional ROIs. Original values of activation size of ROIs were reported. EP = early pubertal adolescent face; LP = late pubertal adolescent face; EA = emerging adult face (peer); PA = parent-aged face condition; FFA = fusiform area; OFA = occipital face area; pSTS = posterior superior temporal sulcus.

one subcategory of faces (e.g., peer faces) was equally selective for other subcategories of faces. Importantly, although the ROI was defined using the core subcategory (e.g., peer faces – objects), the important and independent information is regarding the contrast in magnitude between core and other subcategories of faces. Because the other subcategories of faces were not used to define the ROI, this is an independent analysis. As with the behavioral data, we computed a measure of "other faces" by averaging the beta weights from the four other face subcategories to compare to the core/defining category of the ROI. Because this was a planned contrast, we used paired-samples *t* tests to evaluate the difference in magnitude of activation in each ROI and the 95% confidence intervals of the difference scores. This also reduced the number of statistical tests we administered per ROI, which reduced the FWE rate. In the ROIs, we executed each of these contrasts (e.g., peer–other; child–other) separately. As a result, we employed a Bonferroni correction for the number of contrasts within each ROI (0.05/5, $p = .01$) to these analyses.

Face recognition task. Within each participant, an ROI-based GLM was computed on the time-series data from the fMRI face recognition task in the individually defined right and left FFA1 ROIs (for each face subcategory) obtained from the visual stimulation task. This generated a set of beta weights for each face subcategory for each participant (child, EP adolescent, LP adolescent, peer, and PA faces). As in analyses of the data from the visual stimulation task, we computed a measure of "other faces" by averaging the beta weights from the nondefining face subcategories. We submitted the beta weights from the defining and "other face" categories to separate paired-samples t tests for each ROI to evaluate the relative selectivity of each ROI to the defining face category. These were planned contrasts that reduced the number of statistical tests we administered per ROI, and thus, the FWE rate. Relations between the neural magnitude and behavioral performance in fMRI face recognition task for each face subcategory were explored using linear regression analyses with neural magnitude (i.e., beta weight) as independent variable and behavioral performance as the dependent variable in separate analyses. All the results were Bonferroni corrected for the number of contrasts within each ROI.

RESULTS

Behavioral Results

Peer Bias Task

Figure 1B illustrates performance in the peer bias face recognition task as a function of face subcategory. To evaluate the replicability of our previous findings, peer faces were initially contrasted with "other faces" as defined by the average performance (i.e., d') in response to the child and adolescent faces (see Picci & Scherf, 2016). The planned contrast revealed a peer bias, $t(130) = 3.20$, $p < .005$ (1-tailed; 95% CI of the difference = [0.08, 0.35]), indicating enhanced recognition of peer ($M = 0.85$, $SE = 0.06$) compared with other ($M = 0.71$, $SE = 0.05$) faces. Second, when "other faces" included PA faces as well, the analyses also revealed a peer bias, $t(130) = 2.06$, $p < .05$ (1-tailed; 95% CI of the difference = [0.08, 0.28]), with superior recognition of peer compared with other ($M = 0.63$, $SE = 0.05$) faces. There were no other subcategories of faces that evinced this privileged status for adults. In other words, adults performed similarly when comparing each of the other subcategories of faces to the other groups of faces. Together, these results indicate that the subcategory of peer faces is privileged in the face recognition behavior of EAs, even when including the age-related category of faces that are likely to be the most overrepresented in their visual input (i.e., PA faces).

In addition, we analyzed the data from 19 of the 31 individuals who also participated in the fMRI study. We only have partial behavioral data for these individuals who participated in our neuroimaging task because of computer error during data collection. Figure 1C shows scanning participants' behavioral performance in the peer bias face recognition task. For these individuals, the planned contrast also revealed a peer bias in their recognition behavior, $t(18) = 1.89$, $p < .05$ (1-tailed; 95% CI of the difference = [−0.04, 0.75]), indicating enhanced recognition of peer ($M = 1.14$ $SE = 0.18$) compared with other faces ($M = 0.78$, $SE = 0.15$); when "other faces" included PA faces as well, the analyses also revealed a peer bias, $t(18) = 1.87$, $p < .05$ (1-tailed; 95% CI of the difference = [−0.05, 0.85]), with superior recognition of peer compared with other faces ($M = 0.74$, $SE = 0.15$).

fMRI Face Recognition Task

In contrast to the face recognition task outside the scanner, EA participants did not exhibit a peer bias in face recognition behavior during the 1-back fMRI face recognition task. They exhibited equal recognition of peer faces ($M = 0.98$, $SE = 0.01$) and other-aged faces ($M = 0.97$, $SE = 0.01$), $t(29) = 1.88$, $p = .07$ (1-tailed; 95% CI of the difference = [−0.001, 0.02]), which is not surprising given that performance for all conditions was at ceiling.

Neuroimaging Results

Visual Stimulation Task

Tables 2–3 illustrate the number of participants for whom each ROI was functionally definable and the average coordinates of the centroid of each ROI across participants. To maximize power in our analyses, we only quantified data from ROIs in which at least 50% of the participants (i.e., 16 out of 31) exhibited definable activation. Therefore, we excluded bilateral ATL, amygdala, and left OFA and left pSTS from subsequent analyses.

Number and location of definable face-related ROIs. We used the nonparametric Friedman test to evaluate whether there were differences in the numbers of participants who exhibited definable activation for each ROI as a function of each face subcategory (e.g., FFA1 child faces vs. adolescent vs. peer vs. PA faces). There were no significant differences in the numbers of definable ROIs across face subcategories in any of the ROIs (all $p > .05$). In other words, within each face-selective ROI (i.e., rFFA1, lFFA1, rOFA, rpSTS), if a participant evinced face-selective voxels for any one face subcategory (e.g., child faces), they likely had face-selective voxels for each of the other face subcategories as well (i.e., adolescent, peer, parent).

Following Scherf, Luna, Minshew, and Behrmann (2010), we also tested whether there is a difference in the location of the centroid of the face-subcategory ROIs

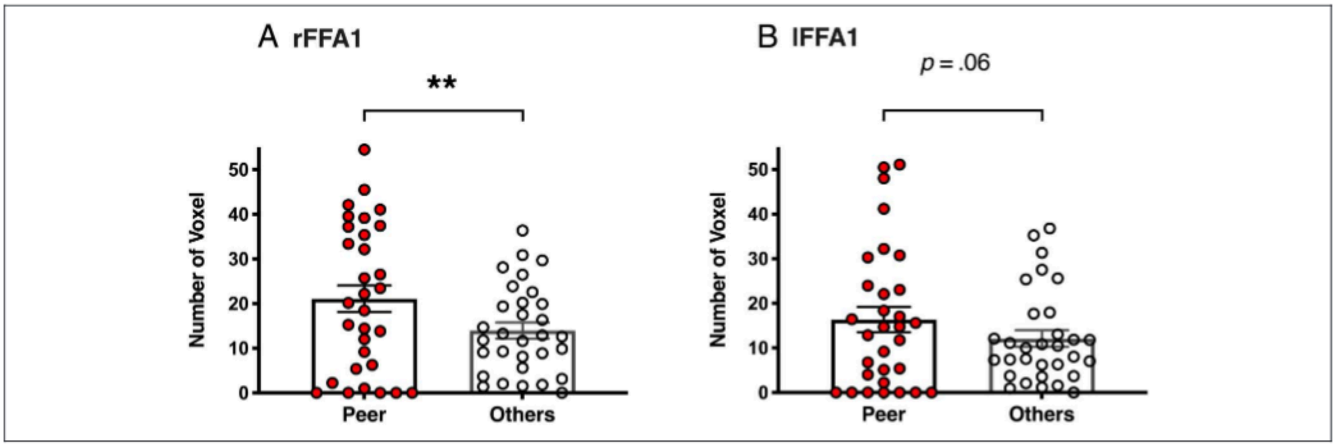

Figure 3. The neural size of peer face FFA1 is larger than that of other subcategory face regions. Within right and left FFA1, separate ROIs were individually defined for each participant for each face subcategory (e.g., peer faces – objects, child faces vs. objects). The plot represents the mean number of contiguously activated voxels in the region ± 1 *SE*. Only the peer face ROIs were significantly larger in the right (A) and left (B) FFA1. * $p < .05$. ** $p < .01$. *** $p < .005$ (Bonferroni-corrected).

for each part of the network. (i.e., FFA, OFA, STS). We found that within each region, the subordinate-level face-selective ROIs were highly overlapping.

Size of definable ROIs. Within each of the individually defined face-selective ROIs (e.g., rFFA1), we investigated whether the separate ROIs for each face subcategory differed in size (i.e., number of significantly active contiguous voxels). Means and standard errors of ROI size for each definable ROI are shown in Table 3. We observed a difference in the size of the functionally defined face regions bilaterally within left and right FFA1 (see Figure 3). In lFFA1, peer faces elicited a larger swath of activation than did the other face categories, $t(30) = 2.19$, $p = 0.06$ (1-tailed; $M_{\text{peer}} = 16.36$, $SE = 2.83$; $M_{\text{other}} = 12.09$, $SE = 2.13$; 95% CI of the difference = [0.03, 0.74]). Similarly, in rFFA1, peer faces elicited a larger swath of activation than did the other face categories, $t(30) = 2.92$, $p < .001$ (1-tailed; $M_{\text{peer}} = 21.07$, $SE = 2.81$; $M_{\text{other}} = 13.96$, $SE = 2.32$; 95% CI of the difference = [0.14, 0.89]). Results are Bonferroni corrected for the number of ROIs ($p = .05/4 = 0.0125$). Figure 4 illustrates the subcategory ROIs (each in a separate color) in the bilateral FFA1 in a representative brain. Peer faces also elicited a larger swatch of activation than other face subcategories in both the right OFA and pSTS; however, these results are not statistically significant with correction.

Magnitude of activation within definable ROIs. In these analyses, the comparison of activation in response to different subordinate-level categories of faces was conducted in each basic-level face-defined ROI (e.g., peer faces vs. objects). Importantly, because the ROI is defined relative to objects, the estimation of the neural response to the "other face" categories is of primary interest. The estimation of this response is independent of the voxel selection process. We discuss the significant results here, but the full set of results is reported in Table 4.

Other faces elicited significantly weaker activation than did peer faces in peer-face defined rFFA1, lFFA1, and rpSTS. Other faces also elicited significantly weaker activation than child faces in child-face defined lFFA1. We also found that other faces elicited a significantly weaker activation than

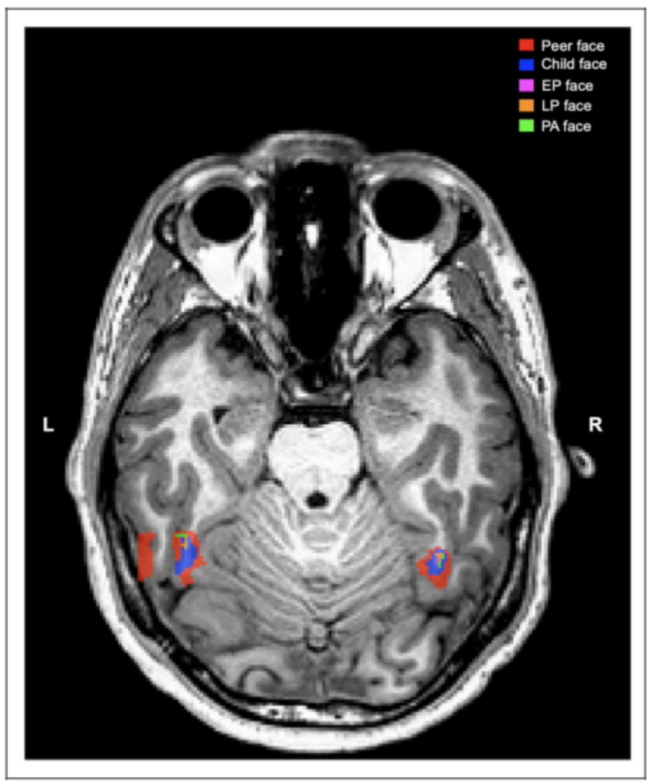

Figure 4. Representative brain activation to face subcategory within bilateral FFA1. A transverse view of brain activation within bilateral FFA from one participant (subject ID: sub_011) is shown. Within the bilateral FFA1, separate ROIs were defined for each face subcategory including peer (i.e., emerging adult), child, early pubertal (EP) adolescent, late pubertal (LP) adolescent, and parent-aged (PA) adult faces. L = left; R = right.

Table 4. Summary of Neural Magnitude Results from Visual Stimulation Task (fMRI)

		Target Faces	Other Faces			
Face Contrast	*ROIs*	*M (SE)*	*M (SE)*	*df*	*t Value*	*95% CIs*
Peer vs. others	rFFA1	0.34 (0.04)	0.17 (0.03)	25	3.70**	[.03, .25]
	lFFA1	0.37 (0.04)	0.21 (0.03)	23	2.90**	[.05, .27]
	rOFA	0.82 (0. 20)	0.77 (0.18)	15	1.06	[−.05, .15]
	rpSTS	0.92 (0.29)	0.74 (0.11)	22	3.00*	[.05, .29]
Child vs. others	rFFA1	0.33 (0.04)	0.22 (0.03)	27	2.35	[.02, .19]
	lFFA1	0.32 (0.04)	0.18 (0.02)	26	3.89***	[.08, .25]
	rOFA	0.91 (0.15)	0.95 (0.13)	14	−.59	[−.18, .10]
	rpSTS	0.74 (0.12)	0.83 (0.14)	20	−1.66	[−.21, .02]
EP vs. others	rFFA1	0.24 (0.03)	0.19 (0.02)	25	−.59	[−.12, .06]
	lFFA1	0.31 (0.02)	0.20 (0.03)	24	2.59*	[.01, .18]
	rOFA	0.84 (0.12)	0.70 (0.16)	15	2.03	[−.01, .29]
	rpSTS	0.83 (0.10)	0.73 (0.13)	22	1.82	[−.01, .21]
LP vs. others	rFFA1	0.33 (0.04)	0.16 (0.03)	26	4.20***	[.07, .25]
	lFFA1	0.36 (0.08)	0.17 (0.03)	25	4.62***	[.11, .30]
	rOFA	1.06 (0.20)	0.93 (0.17)	16	1.97	[−.01, .28]
	rpSTS	0.95 (0.18)	0.69 (0.12)	19	1.81	[−.03, .21]
PA vs. others	rFFA1	0.30 (0.04)	0.20 (0.03)	26	2.58*	[.07, .25]
	lFFA1	0.31 (0.05)	0.20 (0.03)	23	2.97*	[.02, .13]
	rOFA	0.86 (0.18)	0.77 (0.17)	16	1.65	[−.02, .18]
	rpSTS	0.63 (0.03)	0.56 (0.02)	21	.95	[−.05, .14]

CI represents 95% confidence interval. EP = early pubertal adolescent face condition; LP = late pubertal adolescent face condition; peer = emerging adult face condition; PA = parent-aged face condition; FFA = fusiform area; OFA = occipital face area; pSTS = posterior superior temporal sulcus.

* $p < .05$.

** $p < .01$.

*** $p < .005$ (Bonferroni-corrected).

early pubertal adolescent faces in early pubertal adolescent-face defined lFFA1. We also observed that other faces elicited significantly weaker activation than late pubertal adolescent faces in late pubertal adolescent-face defined rFFA1 and lFFA1. Finally, other faces also elicited significantly weaker activation than PA faces in the PA-face defined rFFA1 and lFFA1 (see Figure 5).

We did not observe significant differences in the magnitude of activation between other faces and target faces in the functionally defined rpSTS and rOFA. Furthermore, there were no significant differences in the magnitude of activation between subordinate-level categories of faces in the control regions (i.e., bilateral EVC). These findings suggest that there is a high degree of functional specificity in FFA1 for representing subordinate-level categories of human faces, particularly in terms of developmental stage.

fMRI Face Recognition Task

Magnitude of activation. We focused these analyses on bilateral FFA1 regions where we consistently observed the representations of each face subcategory in the analyses of the visual stimulation task. We discuss the significant results here, but the full set of results is reported in Figure 6 and Table 5.

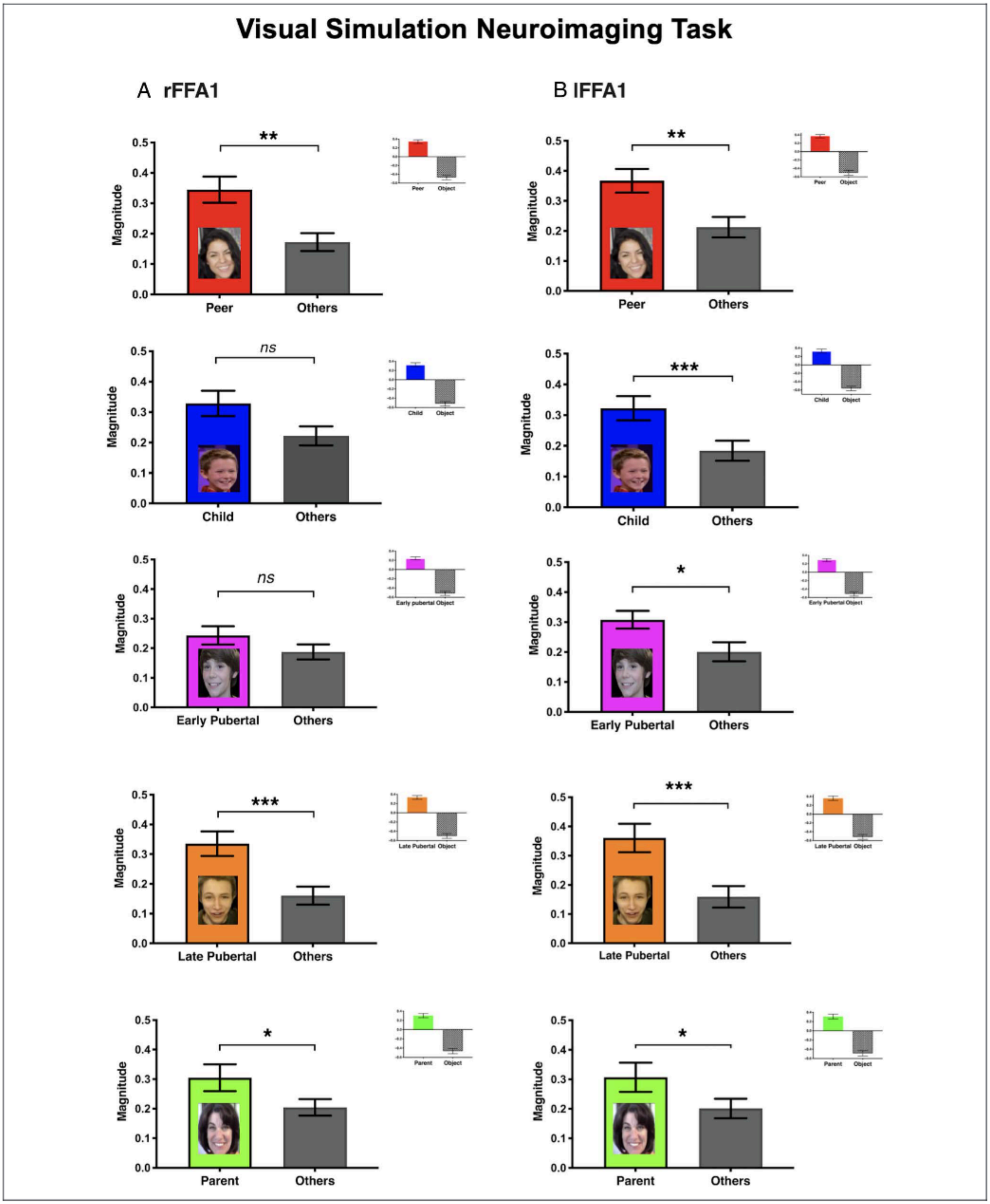

Figure 5. Face subcategory selectivity of ROIs within bilateral FFA1. Within right and left FFA1, separate ROIs were individually defined for each participant for each face subcategory (e.g., peer faces – objects, child faces–objects). To determine the selectivity of these regions, the response to the "other" nontarget faces was evaluated, which is independent from how the regions were functionally defined. Similar magnitude responses would indicate a basic level encoding of faces. In both the right (A) and left (B) FFA1, each of the subcategorically defined face ROIs exhibited a stronger response magnitude to the nontarget faces, indicating a selective response to the target category. Magnitude in the *y* axis represents the beta weight of the BOLD response for each face condition. The plot represents the mean magnitude ± 1 *SE*. * $p < .05$. ** $p < .01$. *** $p < .005$ (Bonferroni-corrected).

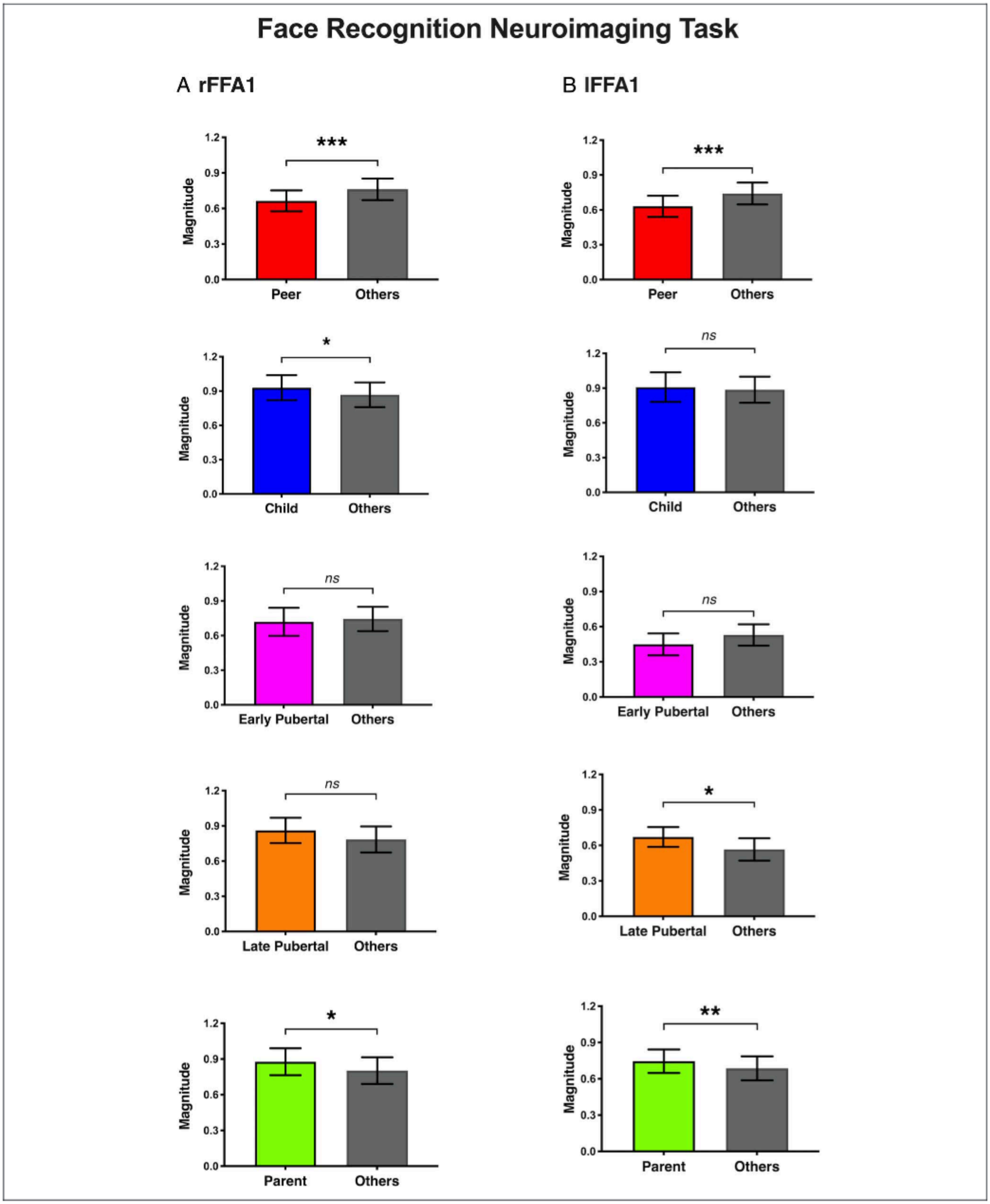

Figure 6. Evaluation of neural response in bilateral FFA1 during face recognition fMRI task. ROI-based GLMs were run on the time-series data from the fMRI face recognition task within the individual-identified regions from the visual stimulation task, and the beta weights were extracted. This allowed us to determine what the neural response of the subcategorically defined regions looked like during the process of recognition specifically. In both the right (A) and left (B) FFA1, the response to peer faces was lower than the response to the other kinds of faces. In all other face subcategory-defined FFA1, the target faces elicited higher activation than did the nontarget faces. The plot represents the means and standard error (*SE*). Magnitude in the *y* axis stands for beta weight for each face condition. * $p < .05$. ** $p < .01$. *** $p < .005$ (Bonferroni-corrected).

Table 5. Summary of Neural Magnitude Results from fMRI Face Recognition Task

Face Contrast	*ROIs*	*Target Faces* *M (SE)*	*Other Faces* *M (SE)*	*df*	*t Value*	*95% CIs*
Peer vs. others	rFFA1	0.66 (0.09)	0.76 (0.09)	25	−3.42***	[−.15, −.03]
	lFFA1	0.63 (0.09)	0.74 (0.09)	23	−4.00***	[−.17, −.04]
Child vs. others	rFFA1	0.94 (0.11)	0.86 (0.11)	24	2.30*	[0, .11]
	lFFA1	0.88 (0.14)	0.86 (0.13)	25	.79	[−.04, .08]
EP vs. others	rFFA1	0.72 (0.13)	0.74 (0.11)	26	−1.71	[−1.12, 0]
	lFFA1	0.45 (0.09)	0.53 (0.09)	25	−2.18	[−.84, −.09]
LP vs. others	rFFA1	0.86 (0.11)	0.79 (0.11)	26	1.97	[−.01, .21]
	lFFA1	0.67 (0.09)	0.56 (0.09)	25	2.59*	[.01, .13]
PA vs. others	rFFA1	0.88 (0.12)	0.80 (0.11)	26	2.77*	[.02, .13]
	lFFA1	0.74 (0.09)	0.68 (0.09)	23	2.94**	[.02, .10]

CI represents 95% confidence interval. EP = early pubertal adolescent face condition; LP = late pubertal adolescent face condition; peer = emerging adult face condition; PA = parent-aged face condition; FFA = fusiform area; OFA = occipital face area; pSTS = posterior superior temporal sulcus.

* $p < .05$.

** $p < .01$.

*** $p < .005$ (Bonferroni-corrected).

In the peer-defined bilateral FFA1, the response to other faces was stronger than that to peer faces. In all other subordinate-level face-defined ROIs, the response to other faces was weaker than to the target category, including the child, late puberty adolescent, and parent-defined ROIs.

Behavioral correlation. Although there were no differences in recognition behavior for subcategories of faces in the scanner task, we conducted exploratory analyses to evaluate potential associations between neural activation and face recognition performance for each subordinate-level category of faces. For each subcategory of face, we computed a separate regression of the difference score in neural magnitude (e.g., peer vs. other faces) on the difference score in face recognition behavior (e.g., peer vs. other faces) for the FFA ROIs. There were no significant relations between neural magnitude and recognition behaviors in any ROI.

DISCUSSION

The psychological relevance of subordinate-level categories of human faces, like race, gender, and developmental stage, is well established behaviorally, and is important for understanding the way we process social categories. Yet, the mechanisms by which the brain represents this subordinate-level information about faces remains largely unknown. The patterns of bias in face recognition behavior reflect differential sensitivity to this subordinate-level information. For example, as children become adolescents, the relatively enhanced ability to recognize adult faces (i.e., caregiver bias) undergoes a developmental change so that peer faces of a similar pubertal status become the privileged subcategory for recognition (i.e., peer bias; Picci & Scherf, 2016). The peer bias becomes even more strongly entrenched in the face recognition behavior of EAs. Our goal in this study was to evaluate the neural mechanisms that represent this kind of subordinate-level information about faces, specifically the primacy of peer faces for EAs, individuals 18–25 years of age who are in a distinct developmental stage in which peers are highly relevant to their social developmental tasks (Arnett, 2000, 2007, 2014).

First, we tested a large cohort of participants in a behavioral paradigm to replicate and extend previous findings of a peer bias in the face recognition behavior of EAs. Then, in a subset of these same participants, we used fMRI to evaluate multiple potential mechanisms by which subordinate-level information underlying the peer bias may be represented within the face-processing neural network. We mapped out the topography of the regions selectively responsive to the five subcategories of faces (child, early puberty adolescent, late puberty adolescent, EA, and parent faces) in each individual participant using a visual stimulation task. This allowed us to evaluate whether the locus, size, or magnitude of activation differentiated each of the subcategories of faces in the face-processing network. Next, we independently interrogated the response properties of these regions as participants engaged in a 1-back face recognition task with all five subcategories of faces.

Emerging Adults Are Biased to Recognize Peer Faces

To replicate and extend our prior work investigating the influence of developmental stage as a relevant type of subordinate-level information that biases the face recognition behavior of EAs, we employed an old/new recognition memory paradigm. In this task, participants encode and recognize faces from each of five developmental stages. Three of these subcategories of faces (child, early puberty adolescent, and late puberty adolescent) all represent developmental stages that EAs have already lived through themselves. In our prior work using this task, we reported a peer bias in EAs, namely, that recognition behavior was superior in the EA condition compared with all other conditions (Picci & Scherf, 2016). This prior finding underscores the importance of peer faces during this developmental period, supporting the notion that the visuoperceptual system is fine-tuned to subserve social developmental tasks (e.g., bonding with peers for relationships; Scherf et al., 2012). Although, the EA face category represents the EAs' current developmental category, and thus their "peers," EA faces may also be overrepresented in their accumulated visual experience given the role that adult caregivers and teachers play in children's and adolescents' lives. In addition, EA faces are sexually mature and, thus, sexually dimorphic, making them potentially more distinctive than the child and adolescent faces. As a result, we extended this prior work here by including another group of sexually mature adult faces that would control for these alternative explanations. We included PA faces (those between the ages of 40–50 years) because they likely represent the faces that are most overrepresented in EAs' visual experience and that are also sexually dimorphic.

Indeed, we observed that EAs exhibit superior recognition for peer faces compared with all other faces even when PA faces were included in the task. First, this finding replicates our previous finding of a peer bias in EAs (Picci & Scherf, 2016). Importantly, it also extends these earlier findings by ruling out alternative mechanistic explanation for the development of this bias (accumulated experience), suggesting that developmental stage is psychologically relevant information that organizes and influences subordinate-level face recognition behavior, which ultimately manifests in the differential sensitivity to peer faces in EAs.

It is important to consider potential alternative explanations for this pattern of findings. For example, there may be something inherently different about the EA faces that make them more memorable or distinguishable in this paradigm than are the other faces. If this is the case, we might predict that a bias for the EA faces would materialize for all groups of participants who take this task. In fact, this is not the pattern of result that we observe. In a prior experiment using these same stimuli (apart from the PA stimuli), adolescent participants were not biased to remember the EA faces. They were biased to remember adolescent faces that matched their own pubertal status. In fact, they evinced a relative decrement in performance on the EA faces (Picci & Scherf, 2016). Therefore, given this pattern of results across studies, it is unlikely that the findings are related to unique characteristics of the EA face stimuli.

Importantly, although this behavioral finding is consistent with the notion of "own-age" bias (Anastasi & Rhodes, 2005), we suggest that when interpreted in the context of the broader set of findings in the literature, it is evident that developmental stage, which is correlated with but not limited to age, is the defining feature for this privileged subordinate-level category in face recognition behavior. For instance, our prior findings show that adolescents matched on age exhibit a bias in recognizing other adolescent faces with whom they share a similar pubertal status (early vs. late), indicating that pubertal status is relevant for defining "peer" faces for adolescents (Picci & Scherf, 2016). Moreover, peer biases do not influence the face recognition abilities of children; instead, they exhibit caregiver biases indicating the primary role of caregivers in their social developmental tasks (for a review, see Scherf & Scott, 2012). In addition, our finding that EAs exhibit a peer bias in their face recognition behavior even when considering parent, adolescent, and child faces together suggests that cumulative visual experience (as represented by parent faces) and lived experiences (as represented by child and adolescent faces) are not the only features for organizing subcategories of faces. The social developmental tasks of the individual, which influence motivational components of face processing (Scherf et al., 2012), are critical as well.

Neural Mechanisms Underlying the Peer Bias in Face Recognition

To investigate the neural mechanisms that subserve the peer bias in EAs' face recognition behaviors, we employed two fMRI tasks. First, we determined whether subordinate-level face categories are represented as separate patches of neural real-estate within the core and/or extended regions of the broader face-processing network. To do so, we employed a visual stimulation task that included blocks of dynamic videos of faces from each of the five subcategories that were all matched on emotional valence. The task also included dynamic videos of common objects.

For each subordinate-level category of face, we individually defined patches of face-selective activation in the bilateral core regions (FFA, OFA, and pSTS) and amygdala and ATL of the extended regions using the contrast (face subcategory – objects). From this set of regions, we were able to quantify separate functional ROIs for each of the face subcategories from at least 50% of the participants in bilateral FFA1, right OFA, and right pSTS. Importantly, if a participant had definable face-selective activation for one of the face categories (e.g., child) within a region (e.g., right FFA), then they were very likely to also have face-selective activation for the other four subordinate-level categories as well. Analyses of the centroid of the location of these subcategory ROIs within each region (i.e., FFA1, OFA, pSTS) revealed that they were, on average, largely overlapping. Therefore, the presence of these subcategory ROIs could mean that the regions are either insensitive to the subordinate-level categories of faces (i.e., respond to faces as a basic level category—anything that has first-order configuration of face features) or that they were exquisitely sensitive to these subordinate levels of categories (i.e., overlapping distributed representations of the developmental stage of human faces). To sort out these possibilities, it was essential that we quantify the size and magnitude of activation for each of the face subordinate-level categories within each region. If the regions are insensitive to face subordinate-level category (i.e., encode faces at the basic level), then the variation in size and magnitude of response across categories is predicted to be very small. If, on the other hand, the regions are differentially sensitive to one subordinate-level category compared with others (e.g., peer faces), then the size and/or magnitude of responses is expected to reflect this sensitivity.

In bilateral FFA1, the size of activation regions for peer faces were larger (~20%), on average, than were the ROIs defined for any of the other faces. The pattern was similar in right OFA and right pSTS, although the findings were not significant. Notably, we did not spatially smooth the data and we identified each functional brain region in each participant based on their own activation patterns and anatomy. When functional data are not smoothed, the size of the area provides critical information about extent of the distributed representation (Golarai, Liberman, Yoon, & Grill-Spector, 2010; Scherf et al., 2007). These findings regarding differences in the size of the peer-defined bilateral FFA1 relative to the other face-defined FFA1 regions are consistent with our previous developmental (e.g., Scherf et al., 2007) and individual differences (Elbich & Scherf, 2017) findings. Specifically, age-related improvements and adult individual differences in face recognition abilities are related to larger face-selective ROIs within the broader face-processing regions, particularly in the bilateral FFA1. We have argued previously that enhanced performance may be reflected in the ability to access more informative or cleaner signal about faces by integrating local circuits that carry information about distributed representations, which presents as a larger single functional ROI at the resolution of fMRI (Elbich & Scherf, 2017). Given the privileged status of peer faces in the face recognition behavior of EAs, these larger functional ROIs for peer faces in bilateral FFA1 might reflect one mechanism by which the brain privileges these representations as well.

We also evaluated whether the magnitude of activation distinguished the encoding and representation of subordinate-level categories of faces. Importantly, only target faces (e.g., peer faces) were used to functionally define the face-selective ROIs. Therefore, assessing the magnitude of response within these ROIs to the nontarget (i.e., other) faces provided an independent assessment of the sensitivity to subordinate versus basic level encoding of faces. A differential response to the nontarget faces would indicate sensitivity to the subordinate-level categories; however, a comparable magnitude response would suggest a more basic level encoding across all the categories. We found that within the peer-defined bilateral FFA1 and right pSTS, nontarget faces elicited significantly weaker activation, indicating sensitivity to the subordinate-level category of peer faces. Furthermore, within each of the other subordinate-level face-selective ROIs of the bilateral FFA1 (child, early puberty adolescent, late puberty adolescent, parent), the nontarget faces also elicited weaker activation within the ROI. Importantly, there were no differences in the profile of activation to any of the subordinate levels of face category in EVC (i.e., no sensitivity to subcategory). This helps rule out concerns that the responses in the FFA1 were driven by differences in the stimuli at the level of the visual input. In summary, this converging set of findings suggests that the bilateral FFA1 encodes each of these subordinate-level categories of faces via the magnitude of activation of response.

To further interrogate the patterns of activation to target and nontarget faces within the bilateral FFA1 specifically during face recognition, we used these same regions derived from the visual stimulation task to conduct separate ROI-based GLMs on the time-series data from the fMRI face recognition task. This approach allowed us to extract beta weights for each subordinate-level face category during the fMRI face recognition task. The voxel selection and estimation of the difference between target and nontarget faces are completely independent. In contrast to the visual stimulation task, during face recognition, when peer faces were the target face, they elicited weaker activation in comparison to the nontarget other faces in bilateral FFA1. This pattern of results was specific to peer faces. When any of the other subordinate-level categories of faces were the target face (for defining the ROI), they elicited stronger activation in comparison to the nontarget faces in bilateral FFA1. Unfortunately, the exploratory analyses of the brain activation–behavior correspondences did not provide any evidence to help interpret these findings. Perhaps these results reflect the relative ease with which EAs recognize peer compared with other groups of faces. In other words, during the task of recognition, especially a particularly easy task, EAs may not have to recruit much activation from the FFA1 when recognizing peer faces. This interpretation of the findings is consistent with empirical reports of decreased activation in the ventral visual pathway, including FFA, to faces of personal expertise such as familiar faces (Beaton et al., 2009), own-age faces (Golarai et al., 2017), and own-race faces (Herzmann, Minor, & Adkins, 2017; Herzmann, Willenbockel, Tanaka, & Curran, 2011; Natu, Raboy, & O'Toole, 2011). Note that this finding contrasts with the finding that EAs recruit larger regions and more activation while passively viewing the dynamic visual stimulation task. This task is unconstrained and is likely engaging a multitude of processes that are influenced by motivational factors and social developmental tasks (e.g., affect recognition, trait evaluation, identity recognition).

Limitations and Future Direction

In this work, we designed the study specifically to maximize power for univariate analyses of multiple neural mechanisms (size, activation). Our approach and strict analytic criteria resulted in a narrow sampling of regions within this broadly distributed face-processing network to only include bilateral FFA1, right OFA, and right pSTS. Going forward, it will be important to employ techniques that enable rigorous sampling of more regions in the network, including m-fus/FFA2 (Weiner & Grill-Spector, 2015) to evaluate representational capacity for subcategorical information about faces. Second, although each face-selective ROI (e.g., FFA1) was independently defined in our analyses, these subcategorical ROIs are largely overlapping. This suggests that the pattern of activation may help distinguish the representations of face subcategories. In subsequent studies, it will be helpful to use multivariate analyses to investigate potential differences in the way subordinate-level categories of faces are represented (distributed vs. more sparsely) within each of these functionally defined ROIs, particularly within the bilateral FFA1. Third, we used a 1-back recognition task to study the neural basis of these subordinate-level category face representations during recognition. However, participants were at ceiling in their behavioral performance. It will be essential for future studies to engage face recognition behavior during scanning under more rigorous conditions (e.g., 2-back task) to elicit the privileged status of peer faces in recognition behavior. This will provide a more naturalistic state under which to interrogate the neural systems and potentially evaluate brain–behavior associations. Finally, as with so many fMRI studies, it will be important to replicate these findings with a larger sample, other developmental groups (e.g., adolescents), and using newer scan sequences that optimize signal-to-noise ratios in the parts of the face processing system that are vulnerable to artifacts during scanning, like the amygdala and the ATL. Importantly, we did employ multiple strategies for improving statistical power with smaller sample sizes in neuroimaging studies (see Poldrack et al., 2017).

Conclusions

To summarize, we reported three key findings in the current study: (1) EAs exhibit a peer bias in face recognition behavior, which indicates a privileged status for a subordinate-level category of faces that is not predicted on the basis of experience; (2) this privileged status of peer faces is supported by the multimodal neural responses within ventral visual pathway (i.e., FFA1) including neural magnitude and neural size; (3) the FFA1, which is a critical region for face processing, fundamentally underlies the representations of subordinate-level categories of faces, in terms of developmental stage. These findings demonstrate the organizational principles that human ventral visual pathway uses to organize social information at a subordinate level, which is essential for navigating human social interactions.

Acknowledgments

We would like to thank staff from the Social, Life, and Engineering Sciences Center for help in acquiring the neuroimaging data.

Reprint requests should be sent to K. Suzanne Scherf, Pennsylvania State University, 113 Moore Building, University Park, PA, or via e-mail: suzyscherf@psu.edu.

Data Availability Statement

Data and materials can be obtained from the corresponding author upon request.

Author Contributions

Junqiang Dai: Conceptualization; Data collection; Experimental design; Finalizing manuscript; Formal analysis; Writing—Original draft; Writing—Review & editing. K. Suzanne Scherf: Conceptualization; Experimental design; Funding acquisition; Supervision; Writing—Review & editing.

Funding Information

The research was supported by a grant (RO1 MH112573-01) from the NIMH to K. S. S., the Department of Psychology, and the Social Science Research Institute at Penn State University.

Diversity in Citation Practices

Retrospective analysis of the citations in every article published in this journal from 2010 to 2021 reveals a persistent pattern of gender imbalance: Although the proportions of authorship teams (categorized by estimated gender identification of first author/last author) publishing in the *Journal of Cognitive Neuroscience* (*JoCN*) during this period were M(an)/M = .407, W(oman)/M = .32, M/W = .115, and W/W = .159, the comparable proportions for the articles that these authorship teams cited were M/M = .549, W/M = .257, M/W = .109, and W/W = .085 (Postle and Fulvio, *JoCN*, 34:1, pp. 1–3). Consequently, *JoCN* encourages all authors to consider gender balance explicitly when selecting which articles to cite and gives them the opportunity to report their article's gender citation balance.

Note

1. Note that this hypothesis is not based on age, like those hypotheses suggesting the "own-age" bias. This hypothesis is focused on the relative influence of social developmental tasks. For example, if an emerging adult becomes a parent, their social developmental tasks shift to caregiving. We predict that the biases in face processing will shift as well to reflect the developmental focus on caregiving. The participants in this study were all recruited from a residential college campus and were not likely to be in caregiving positions. This also explains why the age range of the participants was so narrow.

REFERENCES

Anastasi, J. S., & Rhodes, M. G. (2005). An own-age bias in face recognition for children and older adults. *Psychonomic Bulletin & Review*, *12*, 1043–1047. https://doi.org/10.3758/bf03206441, PubMed: 16615326

Arnett, J. J. (2000). Emerging adulthood: A theory of development from the late teens through the twenties. *American Psychologist*, *55*, 469. https://doi.org/10.1037/0003-066x.55.5.469, PubMed: 10842426

Arnett, J. J. (2007). Emerging adulthood: What is it, and what is it good for? *Child Development Perspectives*, *1*, 68–73. https://doi.org/10.1111/j.1750-8606.2007.00016.x

Arnett, J. J. (2014). Presidential address: The emergence of emerging adulthood. *Emerging Adulthood*, *2*, 155–162. https://doi.org/10.1177/2167696814541096

Arrington, M., Elbich, D., Dai, J., Duchaine, B., & Scherf, K. S. (2022). Introducing the female Cambridge Face Memory Test–Long form (F-CFMT+). *Behavior Research Methods*, 1–14. https://doi.org/10.3758/s13428-022-01805-8, PubMed: 35194750

Beaton, E. A., Schmidt, L. A., Schulkin, J., Antony, M. M., Swinson, R. P., & Hall, G. B. (2009). Different fusiform activity to stranger and personally familiar faces in shy and social adults. *Social Neuroscience*, *4*, 308–316. https://doi.org/10.1080/17470910902801021, PubMed: 19322727

Brigham, J. C., & Malpass, R. S. (1985). The role of experience and contact in the recognition of faces of own- and other-race persons. *Journal of Social Issues*, *41*, 139–155. https://doi.org/10.1111/j.1540-4560.1985.tb01133.x

Cassia, V. M., Picozzi, M., Kuefner, D., & Casati, M. (2008). Short article: Why mix-ups don't happen in the nursery: Evidence for an experience-based interpretation of the other-age effect. *Quarterly Journal of Experimental Psychology*, *62*, 1099–1107. https://doi.org/10.1080/17470210802617654, PubMed: 19142827

Contreras, J., Banaji, M. R., & Mitchell, J. P. (2013). Multivoxel patterns in fusiform face area differentiate faces by sex and race. *PLoS One*, *8* https://doi.org/10.1371/journal.pone.0069684, PubMed: 23936077

Diamond, R., & Carey, S. (1986). Why faces are and are not special: An effect of expertise. *Journal of Experimental Psychology: General*, *115*, 107–117. https://doi.org/10.1037/0096-3445.115.2.107, PubMed: 2940312

Egger, H. L., Pine, D. S., Nelson, E., Leibenluft, E., Ernst, M., Towbin, K. E., et al. (2011). The NIMH Child Emotional Faces Picture Set (NIMH-ChEFS): A new set of children's facial emotion stimuli. *International Journal of Methods in Psychiatric Research*, *20*, 145–156. https://doi.org/10.1002/mpr.343, PubMed: 22547297

Elbich, D. B., Molenaar, P. C. M., & Scherf, K. S. (2019). Evaluating the organizational structure and specificity of network topology within the face processing system. *Human Brain Mapping*, *40*, 2581–2595. https://doi.org/10.1002/hbm.24546, PubMed: 30779256

Elbich, D. B., & Scherf, K. S. (2017). Beyond the FFA: Brain–behavior correspondences in face recognition abilities. *Neuroimage*, *147*, 409–422. https://doi.org/10.1016/j.neuroimage.2016.12.042, PubMed: 27993674

Fox, C. J., Iaria, G., & Barton, J. J. S. (2009). Defining the face processing network: Optimization of the functional localizer in fMRI. *Human Brain Mapping*, *30*, 1637–1651. https://doi.org/10.1002/hbm.20630, PubMed: 18661501

Gauthier, I., Tarr, M. J., Moylan, J., Skudlarski, P., Gore, J. C., & Anderson, A. W. (2000). The fusiform face area is part of a network that processes faces at the individual level. *Journal of Cognitive Neuroscience*, *12*, 495–504. https://doi.org/10.1162/089892900562165, PubMed: 10931774

Gauthier, I., Williams, P., Tarr, M. J., & Tanaka, J. (1998). Training 'greeble' experts: A framework for studying expert object recognition processes. *Vision Research*, *38*, 2401–2428. https://doi.org/10.1016/s0042-6989(97)00442-2, PubMed: 9798007

Genovese, C. R., Lazar, N. A., & Nichols, T. (2002). Thresholding of statistical maps in functional neuroimaging using the false discovery rate. *Neuroimage*, *15*, 870–878. https://doi.org/10.1006/nimg.2001.1037, PubMed: 11906227

Gobbini, M. I., & Haxby, J. V. (2007). Neural systems for recognition of familiar faces. *Neuropsychologia*, *45*, 32–41. https://doi.org/10.1016/j.neuropsychologia.2006.04.015, PubMed: 16797608

Golarai, G., Liberman, A., & Grill-Spector, K. (2017). Experience shapes the development of neural substrates of face processing in human ventral temporal cortex. *Cerebral Cortex*, *27*, 1229–1244. https://doi.org/10.1093/cercor/bhv314, PubMed: 26683171

Golarai, G., Liberman, A., Yoon, J. M. D., & Grill-Spector, K. (2010). Differential development of the ventral visual cortex extends through adolescence. *Frontiers in Human Neuroscience*, *3*, 80. https://doi.org/10.3389/neuro.09.080.2009, PubMed: 20204140

Grill-Spector, K., Golarai, G., & Gabrieli, J. (2008). Developmental neuroimaging of the human ventral visual cortex. *Trends in Cognitive Sciences*, *12*, 152–162. https://doi.org/10.1016/j.tics.2008.01.009, PubMed: 18359267

Grill-Spector, K., Knouf, N., & Kanwisher, N. (2004). The fusiform face area subserves face perception, not generic within-category identification. *Nature Neuroscience*, *7*, 555–562. https://doi.org/10.1038/nn1224, PubMed: 15077112

Grill-Spector, K., & Weiner, K. S. (2014). The functional architecture of the ventral temporal cortex and its role in categorization. *Nature Reviews Neuroscience*, *15*, 536–548. https://doi.org/10.1038/nrn3747, PubMed: 24962370

Havighurst, R. I. (1972). *Developmental tasks and education* (3rd ed.). McKay.

Haxby, J. V., Hoffman, E. A., & Gobbini, M. I. (2002). Human neural systems for face recognition and social communication. *Biological Psychiatry*, *51*, 59–67. https://doi.org/10.1016/s0006-3223(01)01330-0, PubMed: 11801231

Haxby, J. V., Hoffman, E. A., Gobbini, M. I., Haxby, J. V., Hoffman, E. A., & Gobbini, M. I. (2000). The distributed human neural system for face perception. *Trends in Cognitive Sciences*, *4*, 223–233. https://doi.org/10.1016/s1364-6613(00)01482-0, PubMed: 10827445

Herrington, J. D., Riley, M. E., Grupe, D. W., & Schultz, R. T. (2015). Successful face recognition is associated with increased prefrontal cortex activation in autism Spectrum disorder. *Journal of Autism and Developmental Disorders*, *45*, 902–910. https://doi.org/10.1007/s10803-014-2233-4, PubMed: 25234479

Herzmann, G., Minor, G., & Adkins, M. (2017). Neural correlates of memory encoding and recognition for own-race and other-race faces in an associative-memory task. *Brain Research*, *1655*, 194–203. https://doi.org/10.1016/j.brainres.2016.10.028, PubMed: 27815095

Herzmann, G., Willenbockel, V., Tanaka, J. W., & Curran, T. (2011). The neural correlates of memory encoding and recognition for own-race and other-race faces. *Neuropsychologia*, *49*, 3103–3115. https://doi.org/10.1016/j.neuropsychologia.2011.07.019, PubMed: 21807008

Hugenberg, K., Young, S. G., Bernstein, M. J., & Sacco, D. F. (2010). The categorization-individuation model: An integrative account of the other-race recognition deficit. *Psychological Review*, *117*, 1168–1187. https://doi.org/10.1037/a0020463, PubMed: 20822290

Kanwisher, N., Tong, F., & Nakayama, K. (1998). The effect of face inversion on the human fusiform face area. *Cognition*, *68*, B1–B11. https://doi.org/10.1016/s0010-0277(98)00035-3, PubMed: 9775518

Kaul, C., Rees, G., & Ishai, A. (2011). The gender of face stimuli is represented in multiple regions in the human brain. *Frontiers in Human Neuroscience*, *4*, 238. https://doi.org/10.3389/fnhum.2010.00238, PubMed: 21270947

Kubota, J. T., Banaji, M. R., & Phelps, E. A. (2012). The neuroscience of race. *Nature Neuroscience*, *15*, 940–948. https://doi.org/10.1038/nn.3136, PubMed: 22735516

Langner, O., Dotsch, R., Bijlstra, G., Wigboldus, D. H. J., Hawk, S. T., & van Knippenberg, A. (2010). Presentation and validation of the Radboud Faces Database. *Cognition & Emotion*, *24*, 1377–1388. https://doi.org/10.1080/02699930903485076

Levin, D. T. (1996). Classifying faces by race: The structure of face categories. *Journal of Experimental Psychology: Learning, Memory, and Cognition*, *22*, 1364–1382. https://doi.org/10.1037/0278-7393.22.6.1364

Lewin, C., & Herlitz, A. (2002). Sex differences in face recognition—Women's faces make the difference. *Brain and Cognition*, *50*, 121–128. https://doi.org/10.1016/s0278-2626(02)00016-7. PubMed: 12372357

LoBue, V., & Thrasher, C. (2015). The Child Affective Facial Expression (CAFE) set: Validity and reliability from untrained adults. *Frontiers in Psychology*, *5*, 1532. https://doi.org/10.3389/fpsyg.2014.01532, PubMed: 25610415

Lundqvist, D., Flykt, A., & Öhman, A. (1998). *Karolinska directed emotional faces*. APA PsycTests. https://doi.org/10.1037/t27732-000

Meissner, C. A., & Brigham, J. C. (2001). Thirty years of investigating the own-race bias in memory for faces: A meta-analytic review. *Psychology, Public Policy, and Law*, *7*, 3–35. https://doi.org/10.1037/1076-8971.7.1.3

Minear, M., & Park, D. C. (2004). A lifespan database of adult facial stimuli. *Behavior Research Methods, Instruments, & Computers*, *4*, 630–633. https://doi.org/10.3758/BF03206543, PubMed: 15641408

Mur, M., Ruff, D. A., Bodurka, J., Bandettini, P. A., & Kriegeskorte, N. (2010). Face-identity change activation outside the face system: "Release from adaptation" may not always indicate neuronal selectivity. *Cerebral Cortex*, *20*, 2027–2042. https://doi.org/10.1093/cercor/bhp272, PubMed: 20051364

Natu, V., Raboy, D., & O'Toole, A. J. (2011). Neural correlates of own- and other-race face perception: Spatial and temporal response differences. *Neuroimage*, *54*, 2547–2555. https://doi.org/10.1016/j.neuroimage.2010.10.006, PubMed: 20937393

Nestor, A., Plaut, D. C., & Behrmann, M. (2011). Unraveling the distributed neural code of facial identity through spatiotemporal pattern analysis. *Proceedings of the National Academy of Sciences, U.S.A.*, *108*, 9998–10003. https://doi.org/10.1073/pnas.1102433108, PubMed: 21628569

Nishimura, M., Scherf, K. S., Zachariou, V., Tarr, M. J., & Behrmann, M. (2015). Size precedes view: Developmental emergence of invariant object representations in lateral occipital complex. *Journal of Cognitive Neuroscience*, *27*, 474–491. https://doi.org/10.1162/jocn_a_00720, PubMed: 25244115

Pascalis, O., & Bachevalier, J. (1998). Face recognition in primates: A cross-species study. *Behavioural Processes*, *43*, 87–96. https://doi.org/10.1016/s0376-6357(97)00090-9, PubMed: 24897644

Pascalis, O., Scott, L. S., Kelly, D. J., Shannon, R. W., Nicholson, E., Coleman, M., et al. (2005). Plasticity of face processing in infancy. *Proceedings of the National Academy of Sciences, U.S.A.*, *102*, 5297–5300. https://doi.org/10.1073/pnas.0406627102, PubMed: 15790676

Picci, G., & Scherf, K. S. (2016). From caregivers to peers. *Psychological Science*, *27*, 1461–1473. https://doi.org/10.1177/0956797616663142, PubMed: 27658903

Pitcher, D., Walsh, V., & Duchaine, B. (2011). The role of the occipital face area in the cortical face perception network. *Experimental Brain Research*, *209*, 481–493. https://doi.org/10.1007/s00221-011-2579-1, PubMed: 21318346

Poldrack, R. A., Baker, C. I., Durnez, J., Gorgolewski, K. J., Matthews, P. M., Munafò, M. R., et al. (2017). Scanning the horizon: Towards transparent and reproducible neuroimaging research. *Nature Reviews Neuroscience*, *18*, 115–126. https://doi.org/10.1038/nrn.2016.167, PubMed: 28053326

Rosch, E. (1978). Principles of categorization. In E. Rosch & B. B. Lloyd (Eds.), *Cognition and categorization* (pp. 27–48). Hillsdale, NJ: Lawrence Erlbaum.

Rosch, E., Mervis, C. B., Gray, W. D., Johnson, D. M., & Boyes-Braem, P. (1976). Basic objects in natural categories. *Cognitive Psychology*, *8*, 382–439. https://doi.org/10.1016/0010-0285(76)90013-x

Scherf, K. S., Behrmann, M., & Dahl, R. E. (2012). Facing changes and changing faces in adolescence: A new model for investigating adolescent-specific interactions between pubertal, brain and behavioral development. *Developmental Cognitive Neuroscience*, *2*, 199–219. https://doi.org/10.1016/j.dcn.2011.07.016, PubMed: 22483070

Scherf, K. S., Behrmann, M., Humphreys, K., & Luna, B. (2007). Visual category-selectivity for faces, places and objects emerges along different developmental trajectories. *Developmental Science*, *10*, F15–F30. https://doi.org/10.1111/j.1467-7687.2007.00595.x, PubMed: 17552930

Scherf, K. S., Elbich, D., Minshew, N., & Behrmann, M. (2015). Individual differences in symptom severity and behavior predict neural activation during face processing in adolescents with autism. *Neuroimage: Clinical*, *7*, 53–67. https://doi.org/10.1016/j.nicl.2014.11.003, PubMed: 25610767

Scherf, K. S., Elbich, D. B., & Motta-Mena, N. V. (2017). Investigating the influence of biological sex on the behavioral and neural basis of face recognition. *ENeuro*, *4*, ENEURO.0104-17.2017. https://doi.org/10.1523/eneuro.0104-17.2017, PubMed: 28497111

Scherf, K. S., Luna, B., Minshew, N., & Behrmann, M. (2010). Location, location, location: Alterations in the functional topography of face- but not object- or place-related cortex in adolescents with autism. *Frontiers in Human Neuroscience*, *4*, 26. https://doi.org/10.3389/fnhum.2010.00026, PubMed: 20631857

Scherf, K. S., & Scott, L. S. (2012). Connecting developmental trajectories: Biases in face processing from infancy to adulthood. *Developmental Psychobiology*, *54*, 643–663. https://doi.org/10.1002/dev.21013, PubMed: 22711622

Scherf, K. S., Thomas, C., Doyle, J., & Behrmann, M. (2014). Emerging structure–function relations in the developing face processing system. *Cerebral Cortex*, *24*, 2964–2980. https://doi.org/10.1093/cercor/bht152, PubMed: 23765156

Stanislaw, H., & Todorov, N. (1999). Calculation of signal detection theory measures. *Behavior Research Methods, Instruments, & Computers*, *31*, 137–149. https://doi.org/10.3758/bf03207704, PubMed: 10495845

Tanaka, J. W. (2001). The entry point of face recognition: Evidence for face expertise. *Journal of Experimental Psychology: General*, *130*, 534–543. https://doi.org/10.1037/0096-3445.130.3.534, PubMed: 11561926

Tanaka, J. W., Kiefer, M., & Bukach, C. M. (2004). A holistic account of the own-race effect in face recognition: Evidence from a cross-cultural study. *Cognition*, *93*, B1–B9. https://doi.org/10.1016/j.cognition.2003.09.011, PubMed: 15110726

Tanaka, J. W., & Pierce, L. J. (2009). The neural plasticity of other-race face recognition. *Cognitive, Affective, & Behavioral Neuroscience*, *9*, 122–131. https://doi.org/10.3758/cabn.9.1.122, PubMed: 19246333

Tanaka, J. W., & Taylor, M. (1991). Object categories and expertise: Is the basic level in the eye of the beholder? *Cognitive Psychology*, *23*, 457–482. https://doi.org/10.1016/0010-0285(91)90016-H

Tottenham, N., Tanaka, J. W., Leon, A. C., McCarry, T., Nurse, M., Hare, T. A., et al. (2009). The NimStim set of facial expressions: Judgments from untrained research participants. *Psychiatry Research*, *168*, 242–249. https://doi.org/10.1016/j.psychres.2008.05.006, PubMed: 19564050

Weiner, K. S., & Grill-Spector, K. (2010). Sparsely-distributed organization of face and limb activations in human ventral temporal cortex. *NeuroImage*, *52*, 1559–1573. https://doi.org/10.1016/j.neuroimage.2010.04.262, PubMed: 20457261

Weiner, K. S., & Grill-Spector, K. (2015). The evolution of face processing networks. *Trends in Cognitive Sciences*, *19*, 240–241. https://doi.org/10.1016/j.tics.2015.03.010, PubMed: 25840651

Wiese, H., Kloth, N., Güllmar, D., Reichenbach, J. R., & Schweinberger, S. R. (2012). Perceiving age and gender in unfamiliar faces: An fMRI study on face categorization. *Brain and Cognition*, *78*, 163–168. https://doi.org/10.1016/j.bandc.2011.10.012, PubMed: 22104172

Whalen, P. J., Johnstone, T., Somerville, L. H., Nitschke, J. B., Polis, S., Alexander, A. L., et al. (2008). A functional magnetic resonance imaging predictor of treatment response to venlafaxine in generalized anxiety disorder. *Biological Psychiatry*, *63*, 858–863. https://doi.org/10.1016/j.biopsych.2007.08.019, PubMed: 17964548

Wright, D. B., Boyd, C. E., & Tredoux, C. G. (2003). Inter-racial contact and the own-race bias for face recognition in South Africa and England. *Applied Cognitive Psychology*, *17*, 365–373. https://doi.org/10.1002/acp.898

Wright, D. B., & Stroud, J. N. (2002). Age differences in lineup identification accuracy: People are better with their own age. *Law and Human Behavior*, *26*, 641–654. https://doi.org/10.1023/a:1020981501383, PubMed: 12508699